Failure Analysis of Various Rolling Mill Equipment at China Steel Corp.

YI-LIANG CHENG*, JEN-HAO HSU* AND TSUNG-FENG WU **

*Plant Engineering & Maintenance Department
** Iron & Steel Research & Development Department
China Steel Corporation

In order to maintain high reliability of all critical equipment during operation, it is important to find out the root cause of the damaged mechanical equipment via all fracture surveys from micro and macro analysis. This could be key to prevention and improvement. This article explains how failure analysis of various rolling mill equipment can be executed by demonstrating two case studies. The first case-study shows a broken mandrel of the pay-off-reel due to a loose mechanical key. The second case-study exhibits a damaged ball joint of the high-pressure descaling system, which could have been triggered by ignored pitting corrosion around its inner surface. It is truly possible to get to the root causes by collecting visual characteristics of fractured surfaces, like beach mark, chevron mark, and T-junction appearance. Which can all directly guide to the initial location of the fracture. It can be further validated by various analytical techniques, such as finite element analysis (FEA), scanning electron microscopy (SEM), energy dispersive spectroscopy (EDS), and backscattered electrons image (BSE) to give credence. Visual examination of a fractured surface at China Steel Corporation (CSC) is one of the engineering problem solving methods to quickly determine the possible cause of almost all damaged mechanical components, provide important clues and diagnostic guidance for troubleshooting. Some special failure modes due to poor design or manufacturing process can then be feedback to newly-produced mechanical equipment, or become bargaining chips against OEM suppliers.

Keywords: Failure analysis, Fatigue, Pitting, Finite element analysis

1. INTRODUCTION

As an integrated steel company, China Steel Corporation (CSC) always puts a lot of effort into keeping a stable operation in all equipment of the manufacturing process from upstream to downstream. However, equipment sometimes fails unexpectedly, so it's necessary to know the cause of the malfunctioning equipment, and make the countermeasure to avoid the same trouble happening again. Equipment failure can be classified as the cause of design, manufacture, operation, or maintenance. But it isn't an easy and effective way in practice to collect all this information, including necessary design drawings, manufacture parameters; monitor sensor data, and maintenance records, to find out the root cause of failure, especially when the parts or components of the equipment fracture. The visual inspection of fractured surface characteristics[1], such as beach marks[2], chevron marks[2], and T-junction appearance[3], is a useful method to trace the initial point of fracture. It can be used to infer the root cause and furthermore be verified by various analytical techniques, such as finite element analysis (FEA), scanning electron microscopy (SEM), energy dispersive spectroscopy (EDS), and backscattered electrons image (BSE) to give credence. This method is executed for equipment troubleshooting in the long term and finding the root cause successfully in CSC. Here are two case studies of rolling mill equipment; the first one is the mandrel of the pay-off-reel, and the other case is the ball joint of the high-pressure descaling system; those demonstrate the failure analysis by the above method.

2. CASE STUDY I

The pay-off reel (Fig.1 (a)), located at the entry section of the strip processing line, unwinds a coil into the downstream line. When the mandrel expands and rotates, the pay-off reel tightens the coil and unwinds the strip to the following equipment. After around 10 years and 7 months of online use, the device cracked at the bolt hole of the key way during normal operation. The broken mandrel was divided into parts A and B for subsequent visual examination. (Fig.1 (b)).

2.1 Visual Examination

The fractured surface of part A was examined, the characteristic beach mark due to fatigue damage was observed (Fig 2 (a)). It can be used to trace the initial crack at the bolt hole in the keyway. The whole fracture surface analysis of the broken mandrel is shown in Figure 2 (b). Inspection of the bolt hole, the thread of this bolt hole was worn (Fig 3 (a)), and the keyway was wider than the original design dimension (Fig 3 (b)).

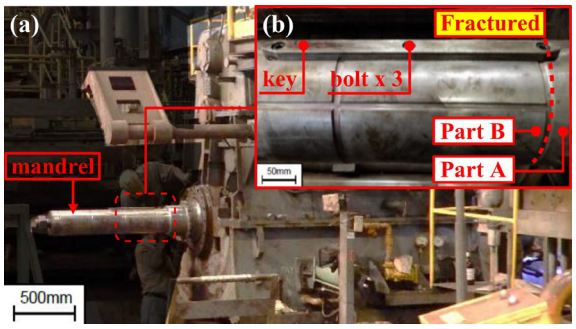

Fig.1. (a) the mandrel position of Pay-Off Reel and (b) fractured position of the mandrel.

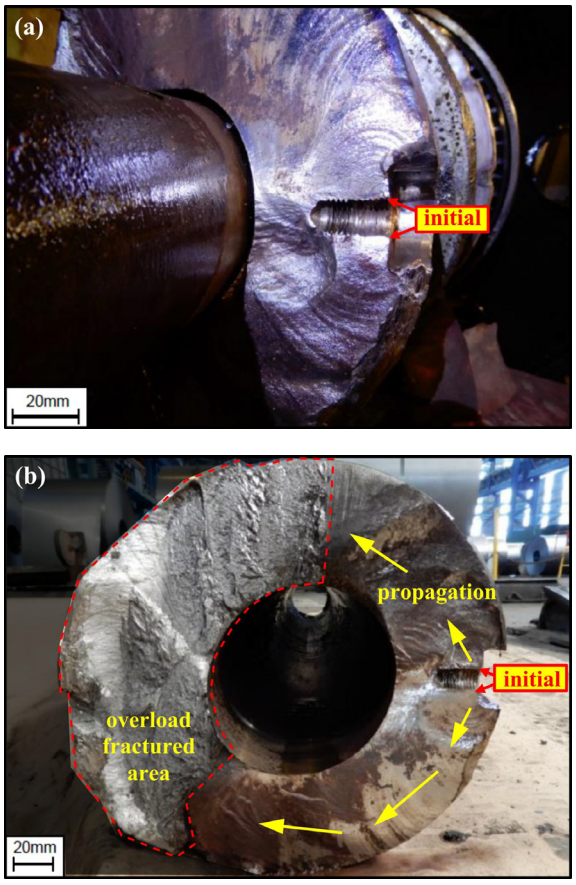

Fig.2. Fractured surface of mandrel (a) part A and (b) part B.

According to this examination, we infer that the mandrel broke as a result of the loosening of the key. The key couldn't be fixed in the keyway since the width of the keyway was wider after long-term service. The force transmission changed from key to bolt due to the above reason and resulted in the bolt hole exerting an abnormal force are shown in Figure 4 (a) and (b).

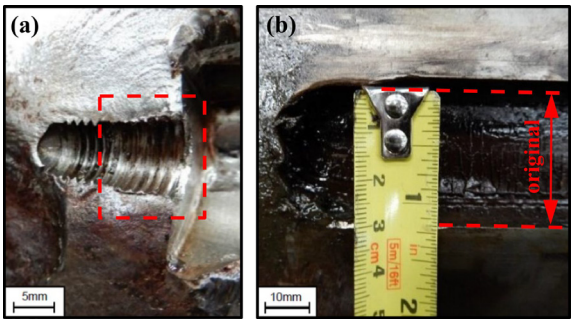

Fig.3. (a) the upper thread of the bolt hole was worn (b) the keyway was wider than the original dimension.

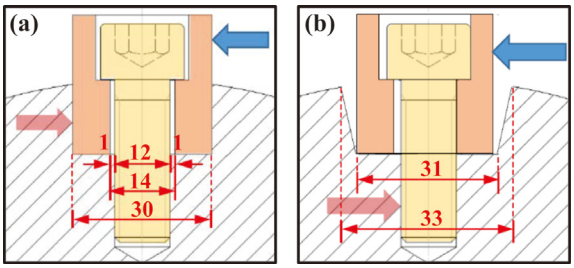

Fig.4. Torque transited (a) by key and (b) by the bo.

2.2 Verification Methodology

In order to verify the inference, we used the finite element analysis software MSC.MARC to create models to simulate the load cases of Figure 4 (a) and (b) respectively, and the results are shown in Figure 5 (a) and (b). In Case I, the maximum equivalent von Mises stress (σ_{VMS}) is located at the fillet of the mandrel, not at the fractured bolt hole. The maximum σ_{VMS} at the bolt hole is 266 MPa, which does not exceed the fatigue safety limit region (OADB) of the mandrel material (SNCM439) drawn by the Goodman diagram method (Fig.6 (a)), so that fatigue damage does not occur. In Case II, the maximum σ_{VMS} is located at the fractured bolt bole, and its value of 680 MPa exceeds the fatigue safety limit region (OADB) and fatigue damage will occur. Therefore, Case II is the same as the inference of visual examination.

2.3 Countermeasures

In this case, after determining the cause of the damage, it is recommended that (1) the user should

perform a penetration test (PT) on the keyway and bolt hole when they replace the mandrel parts every three months, to confirm that there is no initial crack caused by abnormal stress at the bolt hole; (2) check the dimension of the keyway and bolt hole to avoid the same failure occurrence; (3) change the design of the mandrel, including the position of the broken bolt hole to reduce stress concentration, and by adding a second keyway on the opposite side of the existing keyway, so that when the keyway is worn beyond tolerance, the second keyway can be used to extended the service life.

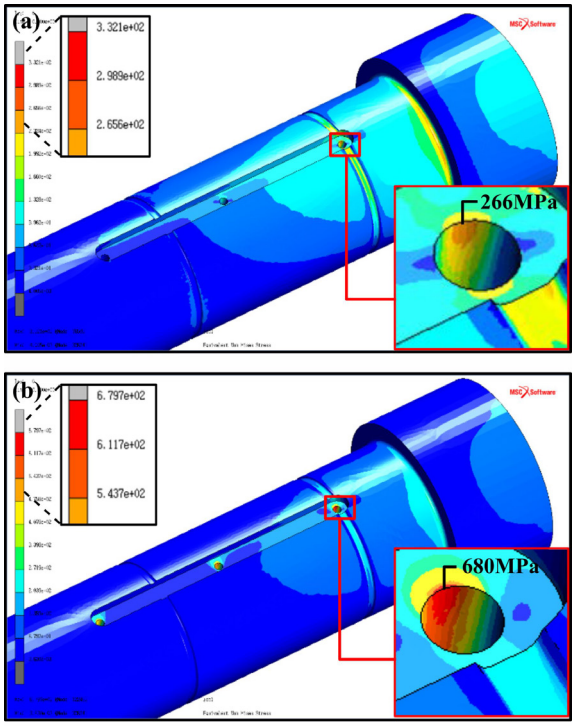

Fig.5. Stress concentration on (a) Case I and (b) Case II.

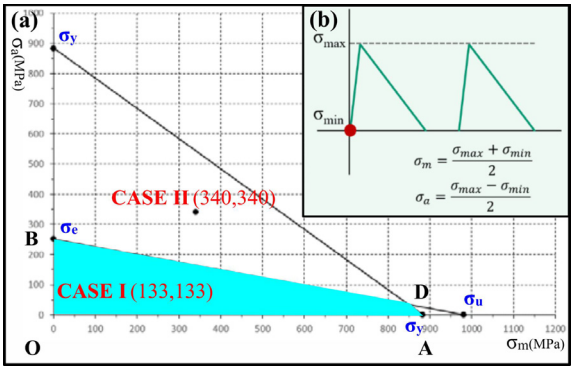

Fig.6. (a) Goodman Diagram[4] and (b) the loading curve of the mandrel.

3. CASE STUDY II

The telescopic tube with ball joint (Fig.7 (a)) of the descaling system is used to transfer the 220-bar of high-pressure water to the downstream nozzles to remove the scale on the hot strip to maintain the high-quality of the strip products. There are four telescopic tubes vertically mounted on the rolling mill, the strip entry and delivery side have two each respectively as shown in Figure 7 (b). One day, the descaling system was alerted to a pressure drop and staff found that the ball joint of the rolling mill entry, operator side was cracked and was ejecting the high-pressure water. After disconnecting the ball joint, it had divided into two pieces (part A and B) as shown in Figure 7 (a). Besides parts A and B, there are two longitude cracks (crack #1 and crack #2) on the ball joint and divide part B into B-1 and B-2, as shown in Figure 8 (a) and (b).

3.1 Visual Examination

Inspecting part B (Fig.9 (a)), it was judged that the left cracked surface (B-1) of part B developed earlier than the right-hand cracked surface (B-2) according to the T-shaped crack generation principle. Figure 9 (b) and (c) zoomed in area of the red framed areas in Figure 9

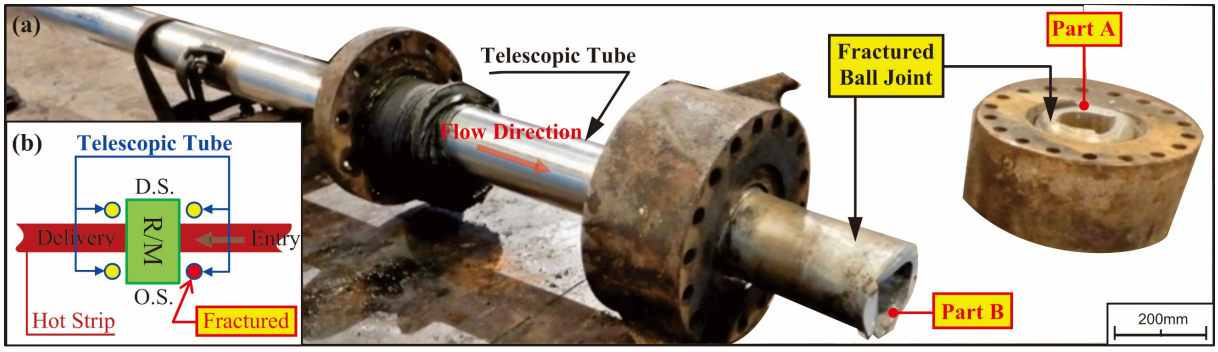

Fig.7. (a) Telescope tube with ball joint and (b) the location of the fractured ball joint.

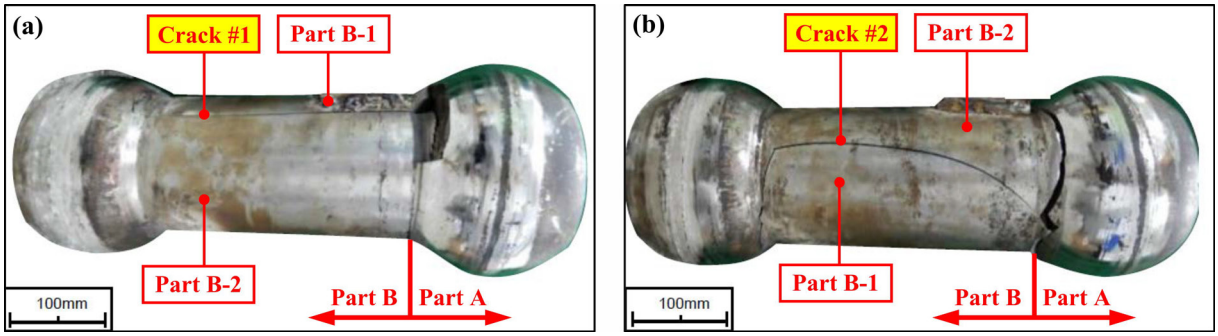

Fig.8. Different views of the fractured ball joint (a) viewpoint 1 and (b) viewpoint 2.

(a); they can be judged as the crack intersection and initial crack of part B's fractured surface respectively, by radial marks. The complete crack propagation of part B's fractured surface is shown in Figure 9 (d).

Figure 10 shows the complete crack propagation analysis of parts B-1 and B-2, the fractured characteristics of A, B, and C areas are shown in Figure 11 (a), (b) and (c) respectively. Combine with the analysis of Figure 9 (d), it can be judged that the fractured ball was initially started at the red ellipse mark of crack #1 in Figure 10, and then propagated toward the upstream and downstream end. In the downstream end, the crack is divided into two directions as shown in Figure 9 (d), the left-hand crack developed earlier and formed crack #2 of parts B-1 and B-2, and the right-hand crack was finally intersected at crack #2.

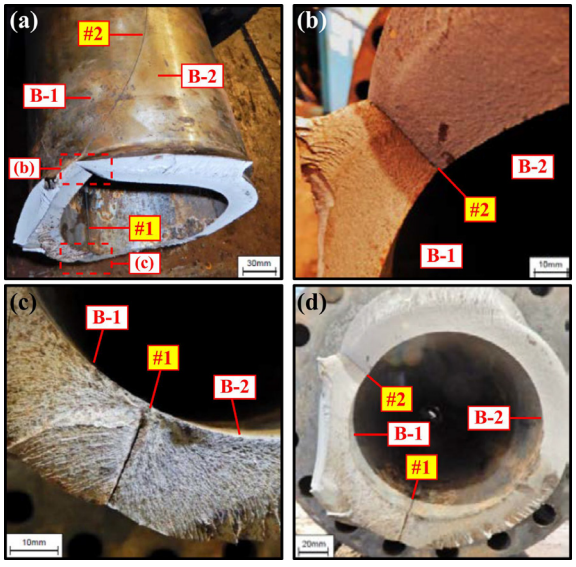

Fig.9. Part B (a) zoomed out view, (b) zoomed in view of the crack intersection, (c) zoom in view of the initial crack, and (d) complete crack propagation.

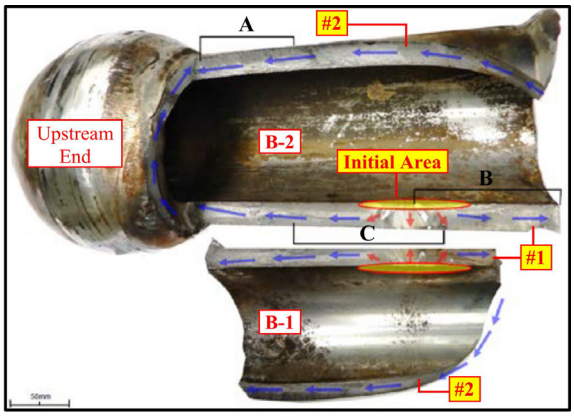

Fig.10. The crack propagation of part B-1 and B-2

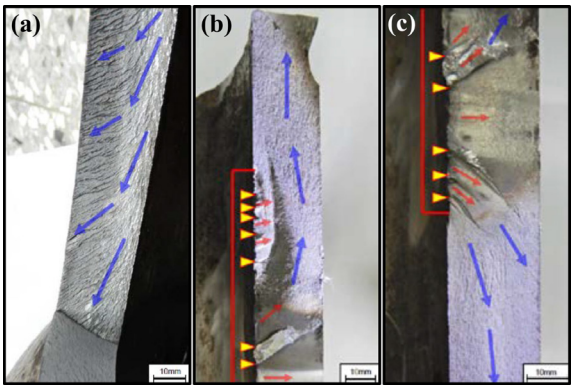

Fig.11. Part B-2 (a) area A, (b) area B, and (c) area C.

The characteristics of pitting corrosion as shown in Figure 12 (a) were found at the inner surface of crack #1 initial area through further inspection. Figure 12 (b) shows the zoomed in red framed area of Figure 12 (a); it showed that the pits near the initial area were connected to form the cracking seams, and the direction of the cracking seams is consistent with the direction of the cracks caused by the pressure.

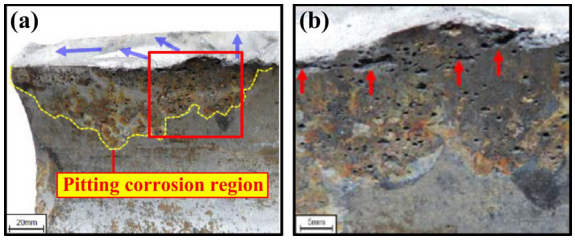

Fig.12. (a) the inner surface of part B-2 initial area and (b) pits form the cracking seam.

According to these findings, we speculated that the pitting corrosion at the inner surface was the root cause of the fractured ball joint. The pits formed the cracking seams under the repeating pressure change while downstream nozzles opened and closed, and then the cracks propagation resulted in eventual fractured.

3.2 Verification Methodology

To verify the inferences, different micro-holes of corrosion regions were first observed by SEM and BSE as shown in Figure 13 (a) to (d). It can be clearly observed that the eroded part of the micro-holes is different in color from the original material, which means that the microstructure of the local area had changed to be very different from that of the original material.

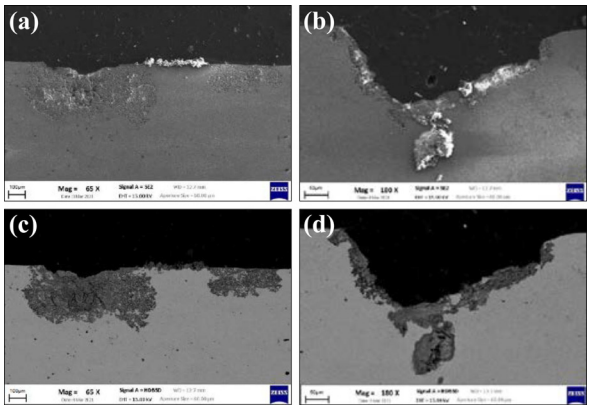

Fig.13. The SEM and BSE image results of two different pitting positions. (a) position 1 SEM, (b) position 2 SEM, (c) position 1 BSE, and (d) position 2 BSE.

The micro composition of different micro-holes of corroded regions were checked by EDS, Figure 14 (a) shows the corrosive element Cl was found at the eroded positions #1 and #2 and wasn't found at the original material position #3. The detailed composition of each position is shown in figure 14 (b) to (d), and it can be confirmed that the micro-holes of corrosion were induced by the element Cl. It is typical pitting corrosion consistent with inference.

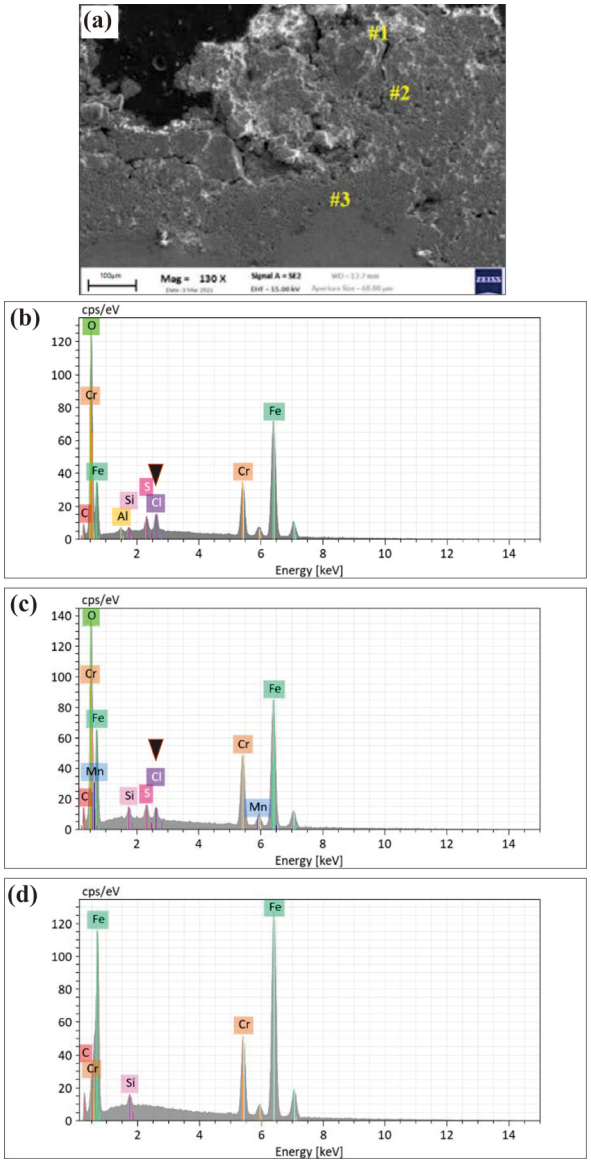

Fig.14. (a) Three testing position at pits and the EDS results for each position. (b) position 1, (c) position 2, and (d) position 3.

3.3 Countermeasures

In this case, it was further confirmed that the composition of the descaling water, especially the corrosive element Cl, was within the control range of the water treatment plant. The ball joint was equipped vertically on the rolling mill, but a longitude corrosion region and deposits were found on the inner surface as shown in Figure 15, which means that the ball joint had corroded when it was placed in a horizontal manner. Since the above finding and the other ball joints didn't rupture. It is speculated that the fractured ball joint was an independent case, it had been polluted before online use

resulting in a local flow field changing occurrence and chloride ion aggregating further.

According to the above analysis and inference, it is recommended (1) prior to use, check if there is any abnormal hole or defect on the inner surface of the ball joint and remove all residuals on the inner surface, such as anti-rust oil, deposits, and rust, to avoid the existence of stress concentration or undesirable factors that cause chloride ion aggregation. (2) During storage, seal the ball joint tightly and store it in a nearly vertical manner to avoid induced corrosion caused by the external environment.

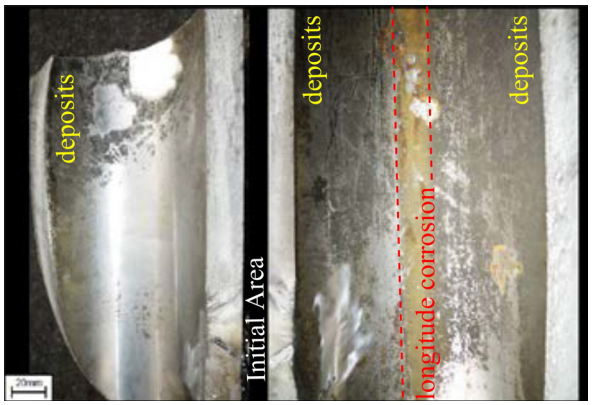

Fig.15. A longitude corrosion region on the inner surface.

4. CONCLUSION

The above two case studies demonstrate the failure analysis manner of the rolling mill equipment in CSC and indicate that the visual examination of a fracture surface can be used as a method to quickly determine the cause of damaged parts, provide important clues, and diagnostic directions for troubleshooting. The verified root cause can be a guide for improving life cycle cost of the equipment, and beneficial when negotiating with the supplier.

REFERENCES

1. Aaron Tanzer, Determination and Classification of Damage, (2002), ASM Handbook V11. Failure Analysis and Prevention, pp. 343-350.
2. Russell A. Lund, Shahram Sheybany, Fatigue Fracture Appearances, (2002), ASM Handbook V11. Failure Analysis and Prevention, pp. 627-640.
3. William T. Becker, Roch J. Shipley, Practices in Failure Analysis, (2002), ASM Handbook V11. Failure Analysis and Prevention, pp. 393-417.
4. Arthur H. Burr, Mechanical Analysis and Design, (1983), Elsevier, New York, pp. 186-220.